The Proton Release Group of Bacteriorhodopsin Controls the Rate of the Final Step of Its Photocycle at Low pH[†]

Sergei P. Balashov,*[,‡] Miao Lu,[‡] Eleonora S. Imasheva,[‡] Rajni Govindjee,[‡] Thomas G. Ebrey,[‡] Beimann Othersen III,[§] Yumei Chen,[§] Rosalie K. Crouch,[§] and Donald R. Menick[§]

Center for Biophysics and Computational Biology and Department of Cell and Structural Biology, University of Illinois at Urbana−Champaign, Urbana, Illinois 61801, and Medical University of South Carolina, Charleston, South Carolina 29425

Received August 10, 1998; Revised Manuscript Received November 17, 1998

ABSTRACT: The factors determining the pH dependence of the formation and decay of the O photointermediate of the bacteriorhodopsin (bR) photocycle were investigated in the wild-type (WT) pigment and in the mutants of Glu-194 and Glu-204, key residues of the proton release group (PRG) in bR. We have found that in the WT the rate constant of O → bR transition decreases 30-fold upon decreasing the pH from 6 to 3 with a pK_a of about 4.3. D_2O slows the rise and decay of the O intermediate in the WT at pH 3.5 by a factor of 5.5. We suggest that the rate of the O → bR transition (which reflects the rate of deprotonation of the primary proton acceptor Asp-85) at low pH is controlled by the deprotonation of the PRG. To test this hypothesis, we studied the E194D mutant. We show that the pK_a of the PRG in the ground state of the E194D mutant, when Asp-85 is protonated, is increased by 1.2 pK units compared to that of the WT. We found a similar increase in the pK_a of the rate constant of the O → bR transition in E194D. This provides further evidence that the rate of the O → bR transition is controlled by the PRG. In a further test, the E194Q mutation, which disables the PRG and slows proton release, almost completely eliminates the pH dependence of O decay at pHs below 6. A second phenomenon we investigated was that in the WT at neutral and alkaline pH the fraction of the O intermediate decreases with pK_a 7.5. A similar pH dependence is observed in the mutants in which the PRG is disabled, E194Q and E204Q, suggesting that the decrease in the fraction of the O intermediate with pK_a ca. 7.5 is not controlled by the PRG. We propose that the group with pK_a 7.5 is Asp-96. The slowing of the reprotonation of Asp-96 at high pH is the cause of the decrease in the rate of the N → O transition, leading to the decrease in the fraction of O.

Bacteriorhodopsin's (bR)[1] proton pump (*1*) includes several crucial steps (for reviews, see *2*−*11*):

$$bR \overset{h\nu}{\rightleftharpoons} K \leftrightarrow L \leftrightarrow M_1 \leftrightarrow M_2 \leftrightarrow N \leftrightarrow O \rightarrow bR$$

The all-trans → 13-cis photoisomerization of the chromophore (*2*−*5*) during bR → K photoreaction initiates changes in the environment of the Schiff base and Asp-85, the key part of its counterion (*12*). This results in the transfer of a proton from the Schiff base to Asp-85 during the L → M transition. At neutral pH, the L → M transition is accompanied by proton release to the extracellular surface of the membrane from some group X while Asp-85 stays protonated (*11*, *13*, *14*). At low pH, proton release is delayed until the very end of the photocycle; it occurs during the O → bR transition (*14*, *15*).

In the second part of the photocycle, the Schiff base is reprotonated during the M → N transition (*3*, *16*) from Asp-96 (*4*, *17*) which is located closer to the cytoplasmic side of the membrane (*18*). This intramolecular proton transport is then followed by proton uptake from the cytoplasmic side and reprotonation of Asp-96 during the N → O transition (*17*, *19*−*23*). In the N intermediate, the chromophore is in the 13-*cis*−15-*anti* configuration (*24*), and Asp-85 is protonated (*25*). In the O intermediate, the chromophore is already in the all-*trans* configuration (*26*), and Asp-85 is still protonated (*19*, *27*). Deprotonation of Asp-85 and intramolecular rearrangements to restore the initial conformation of the pigment occur during the O → bR transition. The proton from Asp-85 is transferred to the PRG (*11*), or if the latter is disabled, the proton is slowly released to the extracellular surface (*14*, *21*).

A mutation of any one of three residues, Arg-82 (*28*−*31*), Glu-204 (*30*−*32*), and Glu-194 (*33*, *34*), inhibits fast proton release at neutral pH and greatly slows proton release from Asp-85. These residues are the key parts of the PRG, which appears to be not a single residue but a complex (*33*) organized into a chain (*34*) or a hydrogen-bonded network

[†] This work was supported by NIH Grant GM52023 (to T.G.E.), DOE Grant 95ER20171 (to R.K.C.), and NSF Grant EPS9630167.

* Corresponding author. Department of Cell and Structural Biology, University of Illinois at Urbana−Champaign, B107 CLSL, 601 S. Goodwin Ave., Urbana, IL 61801. Telephone: (217) 333-2435. Fax: (217) 244-6615. E-mail: sbalasho@uiuc.edu.

[‡] University of Illinois at Urbana−Champaign.

[§] Medical University of South Carolina.

[1] Abbreviations: bR, bacteriorhodopsin; WT, wild type; DA, dark adaptation; PRG and X, proton release group X (*14*). The latter is most likely not a single residue but rather a complex (*33*−*35*, *39*, *40*, *49*) that includes Glu-204, Glu-194, water molecules, and possibly Arg-82.

10.1021/bi981926a CCC: $18.00
Published on Web 01/16/1999

(*35*) of residues in the extracellular channel (*36*−*40*) that catalyzes proton release in bR. The recent X-ray structure determination of bR reveals that the carboxyl oxygens of Glu-204 and Glu-194 are quite close to each other, 4 Å (*39*), which suggests strong interaction between the two groups. In the E204Q (*31, 32, 41*) and E194C/Q (*33, 34*) mutants, the lifetime of the O intermediate is greatly increased. Proton uptake coincides with the formation of O and proton release with O decay (*31, 33, 41*). O decay in the E204Q mutant can be accelerated by azide or other weak acids such as cyanate (*41*), which presumably substitutes for the nonfunctional PRG and catalyzes proton release from Asp-85 to the surface during the O → bR transition.

In this study, we examined several aspects related to the role of the PRG in the catalysis of the reactions in the final segment of the photocycle, the N → O → bR transitions.

(1) Origin of the pH Dependence of O Decay at Low pH. Several studies indicated that the rate of the O → bR transition slows at low pH (*42*−*48*). The reason for this has not been established. Our hypothesis is that it is due to the inability of the PRG to deprotonate at low pH (at pH < pK_a of PRG in O). This should result in a slowing of the deprotonation of Asp-85 and O decay. From our studies of the pH dependence of the DA and of the titration of Asp-85, we found that the pK_a of X is about 4.8 in the blue membrane (*28, 49*). Its pK_a in M was determined to be about 5.8 (*14*). At pH < 5, most of the protons from the PRG are not released during the L → M transition because it undergoes only partial deprotonation at a pH < pK_a of 5.8; instead, the protons are released during the O → bR transition (*14*). The pK_a of the PRG in O has not been determined. Our expectation is that it might be close to 4.8 because the O intermediate is structurally similar to the blue membrane. Assuming that deprotonation of the PRG in O facilitates deprotonation of Asp-85 and restoration of the initial state of the pigment, one might expect to observe stabilization (an increase in the lifetime) of the O intermediate at pHs below 4.8. One of the goals of this study was to test this prediction and determine the pK_a of the rate constant of the O → bR transition (and thus presumably the pK_a of the PRG in O) at low pH.

We have examined the pH dependence of O decay in the WT and found that a group with a pK_a of about 4.3−4.5 strongly affects the rate of Asp-85 deprotonation and the O → bR transition. This pK_a is close to the value for the pK_a of the PRG in the blue membrane (4.8). From this, we suggest that the pK_a 4.3 reflects the pK_a of the PRG in O and that this group determines the pH dependence of O decay in the WT at low pH.

(2) Effect of Mutations of Glu-194 on the Rate Constant of O Decay at Low pH. An independent way to test the conclusion that the pK_a of the PRG controls the pH dependence of the O → bR transition is to modify the pK_a of the group by a mutation and then to check if the pH dependence of the O → bR transition is perturbed accordingly. In this study, we used E194D and other Glu-194 mutants in order to test this, because Glu-194 is part of the proton release complex (*33*) and possibly the group on which proton is localized before the release (*34*). We found that the pH dependence of the O → bR transition at low pH is almost abolished in the E194Q mutant, similar to that in the E204Q mutant (*48*).

In the E194D mutant, the pK_a of fast proton release (in M intermediate) is increased to 7.0 from 5.8 in the WT (*34*). If the pK_a of PRG is the major factor that determines the pH dependence of the O → bR transition at low pH, then one might expect that the pH dependence of the rate constant of this transition, k_{ObR}, would be altered in E194D; specifically, its pK_a should be increased. In agreement with this, we found that the pK_a of the pH dependence of the rate constant of O → bR transition in the E194D mutant is increased by more than 1 pK unit compared to the WT. Furthermore, the pK_a of the PRG can be estimated from the pH dependence of DA (*49*). Using this approach, we show that when Asp-85 is protonated (as in the blue membrane and in M and O), the pK_a of PRG is 1.2 units higher in E194D than in the WT. Thus, experiments with the E194Q and E194D mutants provide further evidence that the pK_a of the PRG sets the pH dependence of the O → bR transition at low pH.

(3) The Effect of the E204 and the E194 Mutations on the pH Dependence of the Fraction of O at Neutral pH. It has been known since some of the earliest studies on the photocycle (*42*−*45*) that low pH favors the accumulation of the O intermediate whereas high pH favors the accumulation of the N intermediate, the equilibrium between the two having a pK_a of about 7.2 (*21, 47*). To explain this, it was proposed that the rate of the N → O transition decreases at high pH, presumably because of the slowing of the proton uptake and the reprotonation of Asp-96 (*17, 20*−*22*). In many cases, the decrease in the fraction of O was not accompanied by a decrease in the apparent rate constant of its formation and even was accompanied by the decrease in the rate of its decay (*21, 47, 50*), which made it difficult to provide a straightforward kinetic explanation for the decrease of the fraction of O upon increasing pH. An alternative suggestion was that the state of the PRG might be responsible for the shift of the N ⇔ O equilibrium around pK_a 7 (*21*). If so, then one should expect that in E194Q or E204Q, mutants where this group is disabled, the pK_a of this equilibrium should be greatly altered. We found that this is not the case. In these mutants, as in E194C (*51*), the pK_a of the fraction of O accumulated is in the range of 7.1−7.7, close to that in the WT (7.5). From this, we conclude that it is not the protonation state of the PRG but that of some other residue (presumably Asp-96) which is primarily responsible for the pH dependence of the fractions of N and O intermediates around pH 7. Experiments with the E204Q and E194Q mutants provide clear evidence that it is the decrease in the rate constant of the N → O transition which correlates with the proton uptake that is responsible for the decrease in the fraction of the O intermediate at high pH. We suggest that the fraction of the O intermediate is determined by the rates of reprotonation of Asp-96 and deprotonation of Asp-85 in the N ⇔ O → bR transitions, respectively.

MATERIALS AND METHODS

Purple membrane was isolated from the *Halobacterium salinarium* (formerly *halobium*) strain S9 as described previously (*52*), except that the DNAase treatment was omitted. The construction and expression of the E194D, E194Q, and other mutants in *H. salinarium* was done as described for the R82A mutant (*28*). The absorption spectra

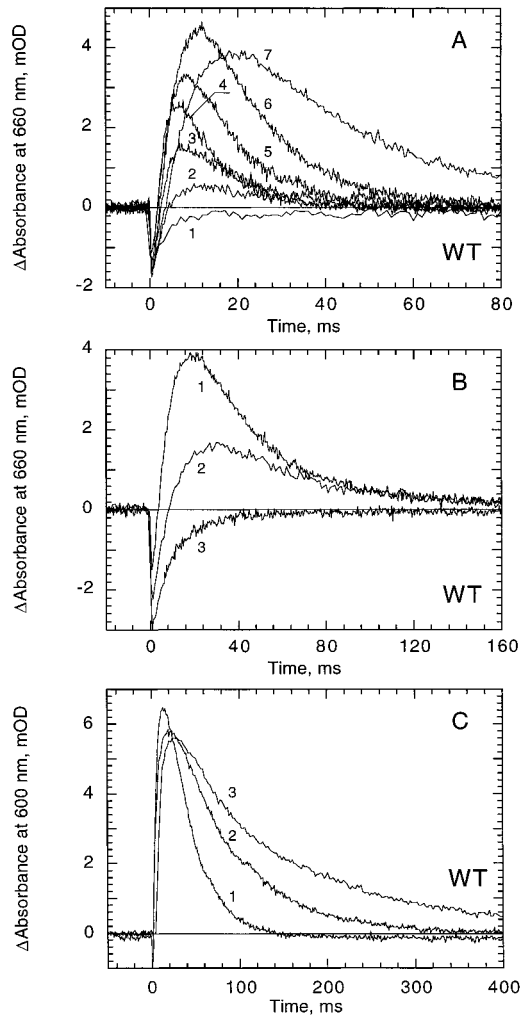

FIGURE 1: Kinetics of the light-induced absorption changes at 660 nm in wild-type bR at 20 °C. (A) Suspension in 75 mM K_2SO_4 at pH 8.6, 8.0, 7.5, 6.9, 4.6, and 4.0 (curves 1−6, respectively); and a gel at pH 3.5 (curve 7). (B) Gels in 75 mM K_2SO_4 at pH 3.5, 3.0, and 2.5 (curves 1−3, respectively). (C) Gels in 4 M KCl at pH 4.0, 3.5, and 3.0 (curves 1−3, respectively).

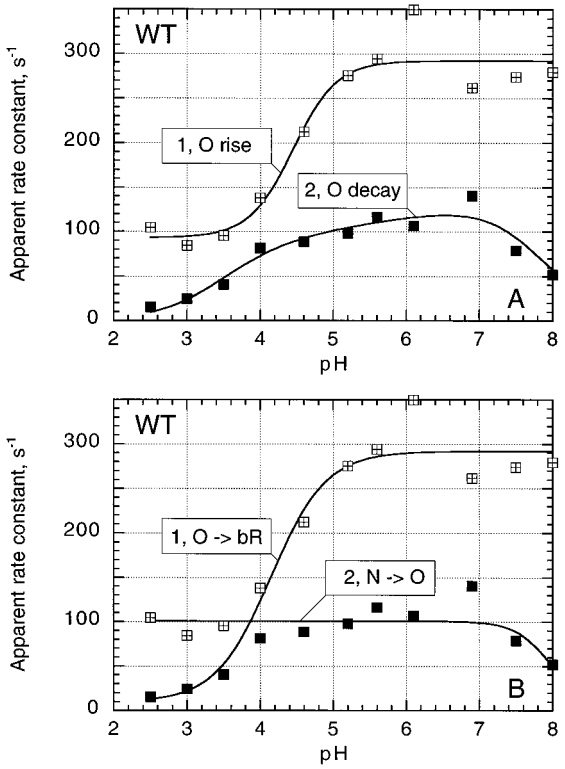

FIGURE 2: (A) pH dependence of the apparent rate constants of O rise (1) and decay (2) in 75 mM K_2SO_4. The constants were obtained from a two-exponential fit of the curves shown in parts A and B of Figure 1. The data were fit by eq 1 (see text). The pK_a for the apparent rate constant is 4.4 for O rise and 3.7 for O decay. (B) Assignment of the rate constants, assuming that the rate of the N → O transition (curve 2) is pH-independent below pH 6 whereas the O → bR transition is faster than the N → O transition at pH 7 and is strongly pH-dependent at lower pH with the pK_a 4.3.

were recorded on a Cary-Aviv 14DS spectrophotometer (Aviv Associates, Lakewood, NJ). The pH titration and DA experiments were performed as described in our earlier studies (*28*, *33*, *49*). Titration of the purple-to-blue transition was done in the dark-adapted samples. The noise in the digital recording of the difference spectra was less than 0.1 mOD. Flash photolysis experiments were done as described previously (*53*). The kinetics of formation and decay of the O intermediate was followed at 660 nm. The kinetic traces at 660 nm were fit into two exponential components using KaleidaGraph (Synergy Software). Mathematica v.3 (Wolfram Research) was used for analytical and numerical solutions of differential equations describing the photocycle reactions. All measurements of photocycle kinetics of O were done at 20 °C on light-adapted samples. For experiments at low pH, acrylamide gels that prevent aggregation at low pH were used. Gels were prepared as described by Liu et al. (*54*), except the purple membrane orientation step was omitted. Gels were incubated at a given pH for at least 12 h. A mixture of six pH buffers (5 mM of citric acid, Mes, Hepes, Mops, Ches, and Caps) was used to stabilize the pH between 11 and 2 for the dark-adaptation experiments. The optical density of the samples for flash-induced absorption changes was 0.3−0.4. D_2O exchange in gels was done by changing solution three times each after 12 h incubation, so that the final concentration of D_2O was more than 97%. DCl was used to adjust the pH (pD). No buffers were used in experiments involving H_2O/D_2O exchange.

RESULTS

pH Dependence of the Accumulation and Decay of the O Intermediate in the WT: Groups with pK_a ca. 7.5 and 4.3 Control Formation and Decay of the O Intermediate, Respectively. Figure 1 depicts the kinetic traces of the light-induced absorption changes at 660 nm in wild-type bR over a pH range from 8.6 to 2.5 in 75 mM K_2SO_4. As one can see from Figure 1, the lifetime of O decay increases at low pH as was found in earlier studies (*42*, *43*, *46*−*48*). The apparent time constant of O decay increases from ca. 10 ms at pH 6 to 40 ms at pH 3.0 (in 75 mM K_2SO_4) whereas the apparent time constant of O rise increases from 3 ms at pH 6 to 10 ms at pH 3. At high salt concentrations (4 M KCl), O decay is slower, but it also experiences a further slowing at low pH (Figure 1C). The kinetic curves of the absorption changes at 660 nm were fitted with two exponentials describing O rise and decay and the apparent rate constants plotted versus pH (Figure 2A). As the pH is lowered, the maximum amplitude of the O intermediate (which is approximately proportional to the absorption changes at 660 nm) increases with a pK_a of ca. 7.5 (Figure 3A) which is close to the earlier reported value of 7.2 in 100 mM Na_2HPO_4

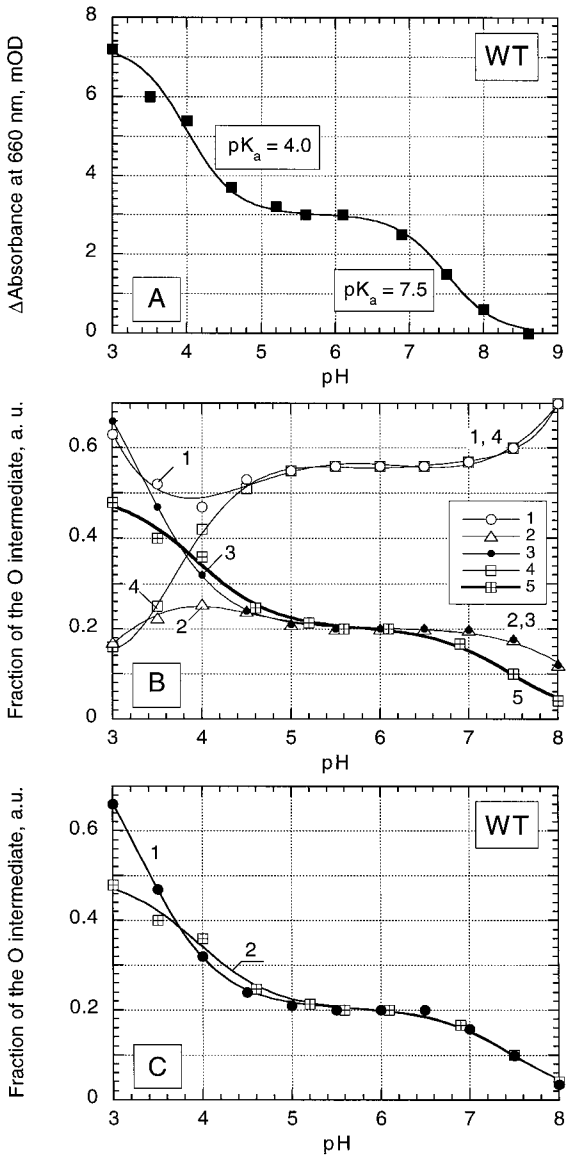

FIGURE 3: (A) The maximum amplitude of the light-induced absorption changes at 660 nm (proportional to the fraction of the O intermediate) in WT bR as a function of pH at 20 °C (in 75 mM K_2SO_4). To account for the decrease in the fraction of pigment cycling due to the purple-to-blue transition at low pH, the data were normalized to the maximum amount of M formed at each pH (at pH 7, the amplitude of M was 20 mOD). (B) Comparison of the pH dependencies of the maximum fraction of O simulated using eq 2 for four different cases (curves 1−4, as described in the text) with the experimental values (curve 5). Curve 5 was obtained from the data shown in Figure 2A, assuming that at pH 6 the maximum fraction of O is 20%, in agreement with the earlier estimates (*46*) and the results of modeling (cases 2 and 3). (C) Comparison of experimental data for the pH dependence of the fraction of O intermediate (curve 2) with a curve simulated assuming that the rate constant of N → O can be approximated as $k_{NO} = 100/(1 + 10^{pH-7.5})$ s^{-1} and the rate constant of O → bR as $k_{O\rightarrow bR} = 300/(1 + 10^{4.5-pH}) + 10$ s^{-1} (curve 1).

(*47*). At lower pHs, we found a further increase with pK_a 4.0 (Figure 3A). Below pH 3.5, the maximal amplitude of O decreases (Figure 1B), mainly because of protonation of Asp-85 in the unphotolyzed state which leads to the transformation of the functionally active purple pigment into the photochemically inactive blue membrane. To account for this effect, the amplitude of O shown in Figure 3A is normalized to the amount of M formed.

To fit the pH dependencies of the apparent rate constants of O rise and decay at low pH (<pH 6) (Figure 2A), we used the following equation:

$$k\,(\mathrm{pH}) = k_0 + k_m/(1 + 10^{pK_a - pH}) \quad (1)$$

The pH dependence of the rate constants in eq 1 is described by a sum of two terms. The first is the pH-independent rate constant k_0. This is the basal rate of O decay (rate of deprotonation of Asp-85) at low pH when the PRG is completely protonated. It is less than or equal to the rate constant observed at pH, below 2.5. The second part of eq 1 is pH-dependent. It is proportional to the maximal rate constant k_m (under conditions in which the PRG can be fully deprotonated, pH 7 for the WT), multiplied by the fraction of the deprotonated residue (presumably the PRG) in the O intermediate with a certain pK_a given by $1/(1 + 10^{(pK_a - pH)})$. The data can be fitted with this equation reasonably well (Figure 2A). The fit gives pK_a = 4.4 ± 0.2 for the rate constant of O rise and pK_a = 3.7 ± 0.2 for the rate constant of O decay. At pH > 7, a decrease in the apparent rate constant of O decay is observed.

Assignment of the Apparent Rate Constants. As a starting point for analysis of the origin of pH dependencies of the apparent rate constants and the fraction of O intermediate, we will use the simple model of two consecutive reactions:

$$(\mathrm{M} + \mathrm{N}) \underset{k_{-1}}{\overset{k_1}{\rightleftharpoons}} \mathrm{O} \xrightarrow{k_2} \mathrm{bR}$$

When the O → N back reaction is negligible ($k_{-1} \ll k_1$), the fraction of O as a function of time is determined by two constants, the rate constant of O formation (k_1) and O decay (k_2) and the fraction of pigment cycling, f (it is assumed in this model that at the initial moment $t = 0$ all pigment cycling is in the precursors of O):

$$f_O(t) = f\,k_1(e^{-k_1 t} - e^{-k_2 t})/(k_2 - k_1) \quad (2)$$

The time when the fraction of O reaches its maximum value is given by:

$$t_{max} = (\ln k_2 - \ln k_1)/(k_2 - k_1) \quad (3)$$

If the pH dependencies of the rate constants are known, the maximum fraction of the O intermediate, f_O^{max}, as a function of pH can be calculated from eqs 2 and 3. In several cases, introduction of a back reaction from O to N (with rate constant k_{-1}) helped to improve the fits. For this case,

$$f_O(t) = f\,k_1/k_3(e^{-k_d t} - e^{-k_r t}) \quad (2')$$

$$t_{max} = (\ln k_r - \ln k_d)/k_3 \quad (3')$$

$$k_r = (k_1 + k_2 + k_{-1} + k_3)/2,$$
$$k_d = (k_1 + k_2 + k_{-1} - k_3)/2,$$
$$\text{and } k_3 = [(k_1 + k_2 + k_{-1})^2 - 4k_1k_2]^{1/2} \quad (4)$$

This model is, of course, a simplification of the photocycle which can be used for the case when M ⇔ N equilibrium is faster than the subsequent N → O and O → bR transitions. For the cases when M ⇔ N equilibrium is slower than the

subsequent reactions, the data were simulated using numerical solutions for the M ⇔ N ⇔ O → bR model.

The apparent rate constants of O rise and decay that are obtained from the fit do not necessarily coincide with microscopic (natural) rate constants of O formation and the O → bR transition. To interpret the pH dependencies of the apparent rate constants shown in Figure 2A, the rate constants should be assigned to the N → O and O → bR reactions. Several possibilities have to be considered. The *first* one is that the apparent constant of O decay (curve 2 in Figure 2A) corresponds to the O → bR transition.

The *second* possible assignment is that the apparent constant of O rise (curve 1 in Figure 2A) corresponds to the rate constant of the O → bR transition whereas the apparent constant of O decay (curve 2 in Figure 2A) reflects the rate constant of conversion of M (through N) into O. This would agree with the suggestion of Gillbro (*55*) for the WT bR at neutral pH that the natural rate constant of O decay is faster than the natural rate constant of O formation, a view also shared by other investigators (*19, 20, 56*). The possibility of such an "inversion" of the rate constants follows from a simple kinetic model of two consecutive reactions. As one can see from eq 2, replacement of k_1 with k_2 and k_2 with k_1 affects the amplitude (maximum fraction) but does not affect the time dependence of the fraction of O. The apparent constant of O decay corresponds to the slowest of the two constants (k_1 and k_2) because the recovery of bR is determined by the slowest reaction in the cycle. Thus, if the rate constant of the N → O reaction k_1 is substantially slower than that of O → bR, k_2, then k_1 appears as the rate constant of O decay.

A *third* way to assign the rate constants is shown in Figure 2B. This interpretation suggests that the rate constant of O formation is pH-independent below pH 6 and equal to ca. 100 s^{-1} (curve 2 in Figure 2B) but that the rate constant of the O → bR transition is strongly pH-dependent; it is faster than the rate of O formation at neutral pH (300 s^{-1} vs 100 s^{-1}) and decreases with pK_a 4.3 upon decreasing pH by at least 30-fold (curve 1 in Figure 2B). Around pH 4, there is a "crossover" of the two constants; below this pH, the rate of O decay becomes the rate-limiting step, and this manifests in the increase in the apparent lifetime of O.

Finally, the *fourth* possibility is opposite to the third assignment; it assumes that the rate constant of the O → bR transition is pH-independent below pH 6 whereas the rate constant of O rise is pH-dependent.

To decide which of the four possible assignments is correct, we generated pH dependencies of the maximum fraction of O accumulated for the four different cases (Figure 3B, curves 1−4) using eq 2 and different combinations of the rate constants. As one can see, case three (Figure 3B, curve 3), which assumes that the rate constant of the N → O transition does not depend on pH below 6 whereas the rate of the O → bR transition is strongly pH-dependent, gives the closest fit of the experimental data (Figure 3B, curve 5). Thus, we conclude that this is the correct assignment of the rate constants.

At pHs above 7, there is a deviation between the fraction predicted by the model and the observed one (Figure 3B). Assuming explicitly that the rate constant of the N → O reaction has pK_a 7.5 and that the pK_a of the rate constant of the O → bR transition is 4.5, we were able to improve the fit of the pH dependence of the maximum fraction of O (Figure 3C) and simulate reasonably well the apparent constants of O rise and decay. Thus, the pH dependence of the rate constant of the N → O transition and a larger rate constant for the O → bR transition than that for the N → O reaction explains the paradox of O (*47, 50*): that the decrease in the fraction of O around pH 7 occurs without a substantial decrease in the apparent rate constant of O rise and even is accompanied by a decrease in the apparent rate constant of O decay.

In summary, the data in Figures 2 and 3 and their fit indicate that the rate constant of the O → bR transition decreases with pK_a ca. 4.3−4.5. We propose that this is the pK_a of the PRG in O (see Discussion). This group in the deprotonated state accepts a proton from Asp-85 and thus facilitates the O → bR transition. At low pH, the fraction of deprotonated PRG decreases and so does the rate of the O → bR transition which results in the accumulation of O.

At pHs above 7, a decrease in the amount of O accumulated is caused by a decrease in the rate constant of O formation. Further evidence for these conclusions was obtained with the E204Q and E194Q mutants.

Evidence That Proton Transfer Is the Rate-Limiting Step in O decay at Low pH: Effect of Azide and D_2O on O Decay at Low pH in the WT. If the hypothesis that the protonation of the group with pK_a ca. 4.5 decreases the rate of proton transfer in the extracellular channel is correct, then one should expect that the addition of azide should accelerate O decay because it was shown that azide facilitates proton transport in the extracellular channel (*57*), particularly under conditions in which the PRG is disabled as in E204Q (*41*). As shown in Figure 4, this effect does take place in the WT at pH 3.2. The lifetime of O decay at pH 3.2 in 250 mM salt is decreased from 37 to 15 ms upon addition of 100 mM azide. An unexpected finding is that azide also accelerates M decay and O formation. M decay speeds up from 11 to 4 ms (Figure 4A) whereas O rise sped up from 9 to 6 ms (Figure 4B). The effect of azide on O decay is much smaller at pH 5 than at pH 3.2 (data not shown). This smaller effect of azide at higher pHs can be explained by assuming that at pH 5 the group with pK_a 4.3−4.5 effectively catalyzes proton release from Asp-85 to the surface so that additional acceleration by azide produces a relatively small increase in the rate. The effect of azide is less pronounced at high salt concentrations. The M decay and O formation do not change with azide whereas O decay is accelerated only slightly from 140 to 100 ms in 4 M KCl (data not shown).

Independent evidence that the slowing of O decay at low pH is caused by a decrease in the rate of proton transfer is the effect of H_2O → D_2O substitution on the kinetics of O decay. As one can see in Figure 5, with H_2O → D_2O substitution, the decay of O slows by a factor of 6.0 ± 0.5 in 150 mM KCl and a factor of 5.0 ± 0.5 in 4 M KCl, suggesting that a proton-transfer reaction is the limiting step in O decay at low pH. The apparent rate constant of O rise is decreased in D_2O by 5.9 times in 4 M KCl. These large D_2O effects on the O rise and decay are similar to that observed for the L → M transition (*58*).

Further Evidence That the O → bR Transition Is Controlled by the PRG: Study of the E194 and E204 Mutants. It has been shown that the E204Q (*31*) and E194C/Q (*33, 34*) mutations dramatically increase the lifetime for Asp-85

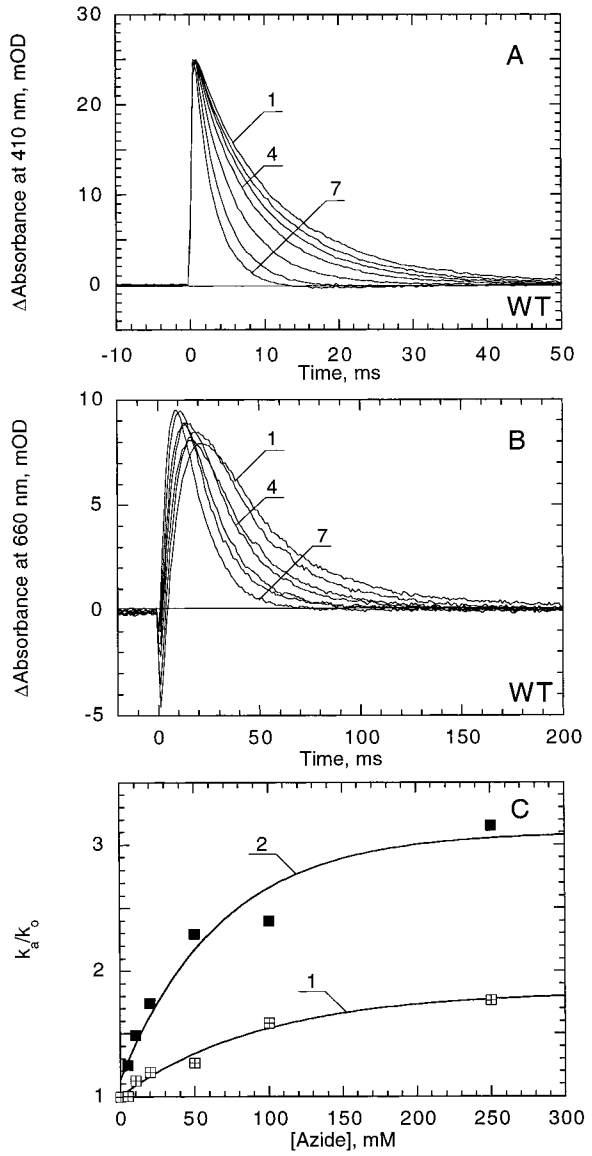

FIGURE 4: Acceleration of photocycle reactions in the WT by azide at pH 3.2. (A) Light-induced absorption changes at 410 nm due to the formation and decay of the M intermediate. (B) Absorption changes at 660 nm due to the formation and decay of the O intermediate. Curves 1−7 in parts A and B correspond to 0, 5, 10, 20, 50, 100, and 250 mM azide, respectively. Aliquots of 250, 245, 240, 230, 200, and 0 mM NaCl were added with the azide to keep the ionic strength constant. (C) Acceleration of the apparent rate constants of O rise (1) and O decay (2) in the presence of azide.

deprotonation (*32*) and O decay. Richter et al. (*48*) have shown that the E204Q mutation completely eliminates the pH dependence of O decay at pH < 6. Here, we investigate the effect of the Glu-194 mutations on the pH dependence of the accumulation of the O intermediate and the effect of these mutations on the ground-state properties of bR: the pK_a of Asp-85 and its coupling with other groups which can be revealed through the titration of the purple-to-blue transition and the pH dependence of the DA.

pH Dependence of the Formation and Decay of the O Intermediate in the E194D Mutant. Dioumaev et al. (*34*) have found that the pK_a of the early proton release that follows M formation is elevated to 7.0 in the E194D mutant (from 5.6 in the WT). Our measurements confirm this result (data not shown). An interesting question is whether the increase in the pK_a of the PRG seen in the M intermediate also persists

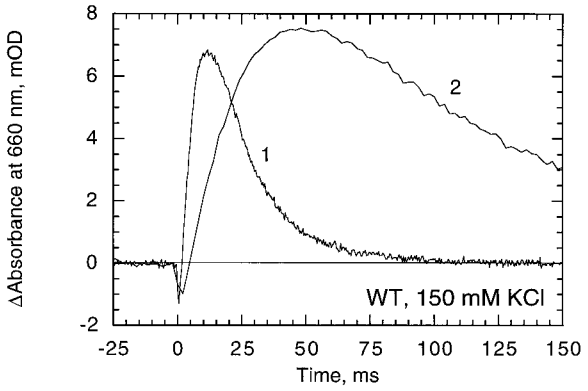

FIGURE 5: The rise and decay of the O intermediate in the WT in 150 mM KCl at pH 3.2 in H_2O (curve 1) and D_2O (curve 2).

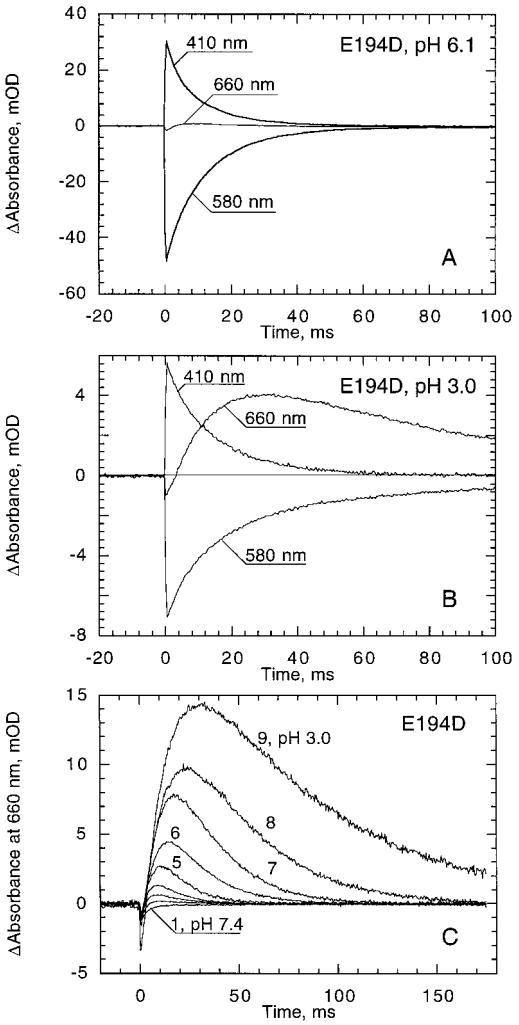

FIGURE 6: Kinetics of light-induced absorbance changes in the E194D mutant in 75 mM K_2SO_4 indicating formation and decay of M (410 nm), bleaching and recovery of bR (580 nm), and O formation and decay (660 nm). (A) pH 6.1. (B) pH 3.0. (C) Traces 1−9 indicate absorption changes at 660 nm at pH 7.4, 6.6, 6.1, 5.6, 5.0, 4.5, 4.1, 3.6, and 3.0. The traces were normalized to the same amount of M formed (for $\Delta A410 = 20$ mOD).

in the O intermediate. That would suggest that the same group that catalyzes proton release in M catalyzes the deprotonation of Asp-85 in the O → bR transition. Figure 6 shows light-induced absorption changes in the E194D mutant at pH 6.1 (panel A) and pH 3.0 (panel B). One can see that only a very small amount of O (relative to the amount of

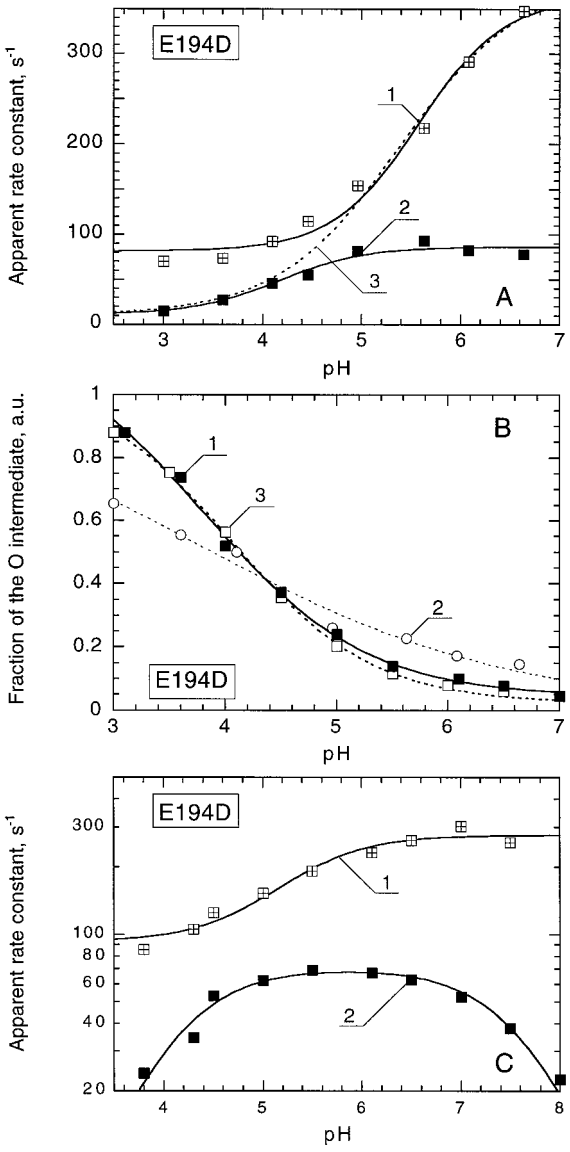

FIGURE 7: (A) pH dependence of the apparent rate constants of O rise (1) and decay (2) in the E194D mutant. The dashed curve (3) shows the pH dependence of the rate constant of the O → bR transition. The curve is fitted with pK_a 5.4. (B) Trace 1, pH dependence of the maximum fraction of the O intermediate in E194D; trace 2 (open circles), simulation using eq 2 and rate constants $k_1 = 80\ s^{-1}$ and $k_2 = 350/(1 + 10^{5.4-pH})\ s^{-1}$; and trace 3 (open squares), simulation using a model M ⇔ N → O → bR, where $k_{MN} = 300/(1 + 10^{(5.3-pH)})\ s^{-1}$, $k_{NM} = 80\ s^{-1}$, $k_{NO} = 60/(1 + 10^{pH-7.5})\ s^{-1}$, and $k_{O\rightarrow bR} = 700/(1 + 10^{5.6-pH})\ s^{-1}$. Note that the p$K_a$ of the maximum fraction of O (ca. 4) does not coincide with the pK_a of the rate constant of the O → bR transition (5.4). (C) pH dependence of the apparent rate constants of M decay in E194D: 1, fast component, and 2, slow component.

M) is accumulated at pH 6.1. A larger amount of O (relative to the amount of M) is accumulated at pH 3. The apparent lifetime of the O intermediate dramatically increases at low pH (see Figure 6C) so that the O → bR transition becomes rate limiting in the recovery of bR. The decay of O is slower than the decay of M (Figure 6B), indicating that back reaction from O → bR, if present, is not significant at low pH. The apparent rate constants of O rise and O decay obtained from the fit are shown in Figure 7A. As in the WT, the best fit of the pH dependence of O amplitude (shown in Figure 7B, curve 1) is obtained by assuming that the rate constant of formation of the O intermediate is pH-independent below pH 6.5 whereas the rate constant of the O → bR transition is strongly pH-dependent (pK_a 5.4), as shown by a dashed line in Figure 7A. The pK_a of the $k_{O\rightarrow bR}$ is more than 1 unit higher than that of the WT (pK_a 5.4 vs 4.3). This shift fits well with the hypothesis that the pH dependence of the O intermediate is controlled by the pK_a of the PRG.

The simulated fraction of the O intermediate in E194D (with the rate constants shown in Figure 7A) is somewhat larger than the experimental data at pH >5 (Figure 7B). The rate constant of the N → O transition has pK_a above 7, as one can see from the fit of O kinetics (Figure 7A). Because the amplitude of O is very small at pH > 6, a more exact determination of the rate constant of N decay can be obtained from the fit of either the pH dependence of bR recovery or the second ("slow") component in M decay. The latter gives a value of 7.5 (Figure 7C), close to that in the WT. Thus, it is not the slowing of the N → O transition but other factors which are responsible for the very small fraction of O in E194D at pH > 6. This can be due to the branching of the photocycle at the N intermediate, so part of the pigment bypasses O during the transformation to bR (*59*). Alternatively, the small fraction of O at neutral pH can also be explained in the framework of the unbranched model of the photocycle (M ⇔ N → O → bR), if it is assumed that the rate constant of the O → bR transition (transfer of the proton from Asp-85 to the PRG), $k_{O\rightarrow bR}$, is substantially larger than the rate constant of the M → O transition (*19*, *20*, *55*, *56*), so the O intermediate does not accumulate. Assuming that the rate constant of the O → bR transition is 700 s^{-1} at pH 7, that it decreases with pK_a 5.6, and that the rate constant of the fast component of M decay changes with pH as shown in Figure 7C (decreases from its maximum value of about 300 s^{-1} with pK_a 5.4), we were able to fit the pH dependence of O (Figure 7 B, curve 3) and quite closely simulate the apparent rate constants of O rise and decay. Thus, the pH dependence of O in E194D can be explained if we assume that the rate constant of the O → bR transition is about 2 times larger than that in the WT and that its pK_a is increased to ca. 5.4−5.6 (from 4.3 to 4.5 in the WT).

Effect of the E194D and E194Q Mutations on the Coupling of Asp-85 and the PRG. Another way to estimate the pK_a of the PRG is based on the titration of Asp-85 either directly or by the measurement of the pH dependence of the rate constant of the DA (*49*); these experiments are described below.

A. Titration and pH Dependence of the DA of the E194D Mutant. The titration curve for the purple-to-blue transition (protonation of Asp-85) in the dark-adapted E194D pigment over a pH range of 2−6 can be fitted with one component with pK_a 3.0 (Figure 8A, open squares); a better fit is obtained with two components with pK_a 2.6 (83%) and pK_a 3.7 (17%). The two pK_a's may be caused by some heterogeneity of the pigment or, alternatively, may be due to an effect of protonation of some residue, Y, on the pK_a of Asp-85. The latter possibility suggests the interaction (coupling) of these two residues. Deprotonation of a residue with pK_a 3.7 causes an increase in the pK_a of Asp-85 by 0.5 units, from 2.6 to 3.1. Note that this is a small pK_a shift compared to a much larger effect which is caused by the deprotonation of the PRG with pK_a 9.1 in the unphotolyzed state as follows from the pH dependence of the DA of E194D (Figure 8A, curve 1).

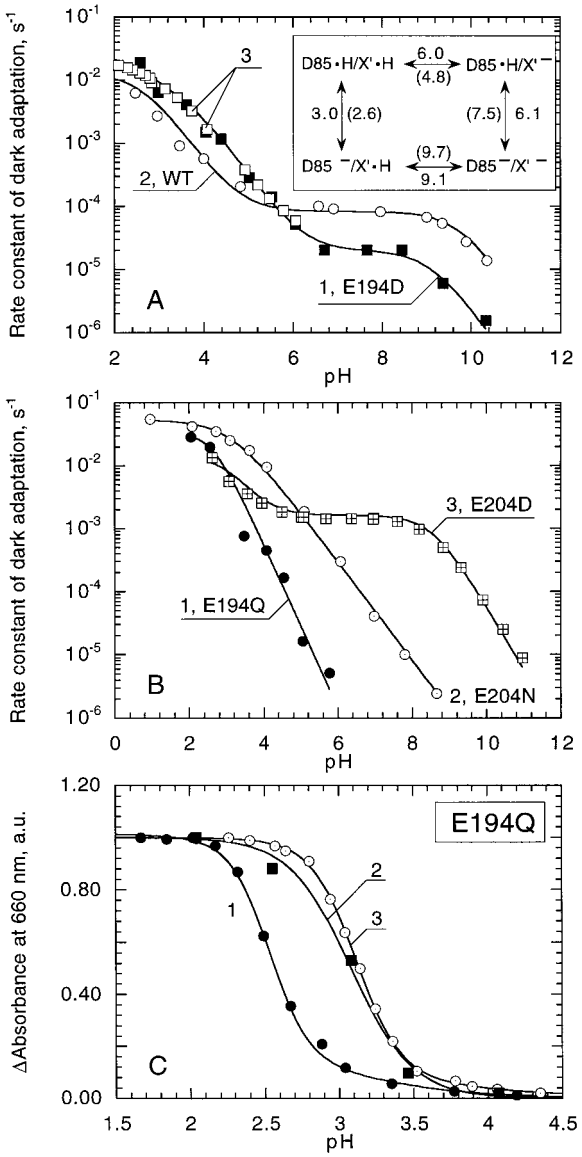

FIGURE 8: (A) pH dependencies of the rate constant of the DA k_{da} in E194D (1) and the WT (2). Open squares (3) indicate the pH dependence of fraction of blue membrane in E194D, normalized with curve 1 in the maximum (at pH 2). The inset shows the pK_a's obtained from the fit of k_{da} for E194D and the WT (in brackets) using an equation derived from the coupling model for Asp-85 and the PRG (*49*). (B) pH dependencies of the rate constants of dark adaptation in E194Q (1), E204N (2), and E204D (3). For curves 1 and 2 the fit is given using the equation $k_{da}(pH) = k_{da}{}^0/[1 + 10^{n(pH-pK_a)}]$; for E204N, the p$K_a$ = 3.1 and n = 0.78, and for E194Q, the pK_a = 2.6 and n = 1.3. The fit for E204D was obtained using the coupling model (*49*, *62*): pK_{a1} = 2.9, pK_{a2} = 8.4, and pK_{a3} = 3.9. Note that the rate constant of thermal isomerization at pH 7 in E204D is 2 orders of magnitude larger than that in E194D, indicating a higher proton affinity of Asp-85 and a larger fraction of the blue membrane at neutral pH, as also shown in ref *34*. (C) Titration of the purple-to-blue transition in E194Q in 75 mM K_2SO_4: 1, a suspension at 20 °C; 2, gels incubated overnight; and 3, a suspension of E194Q at 35 °C.

The pH dependence of the DA in E194D provides information on the coupling of Asp-85 with the PRG because there is a proportionality between the rate constant of the DA and the fraction of blue membrane (*28*, *49*, *62*). This method can also be used in order to decide if a complex titration is caused by the heterogeneity of the pigment or coupling of Asp-85 with some other residue. In the latter case, one would expect that the pH dependence of the DA will be proportional to the fraction of the blue membrane. As shown in Figure 8A, the pH dependence of the DA is proportional to the fraction of the blue membrane in the pH range from 2 to 6 (where the blue membrane could be detected).

Table 1: pK_a of the PRG X and ASP-85 in Different States of the Pigment

pigment	X in M	X in O	X in BM[a]	X in PM[a]	D85 (XH)[b]	D85 (X^-)[c]
WT	5.8[d]	4.3	4.8	9.7	2.6	7.5
E194D	7.0[e]	5.4	6.0	9.1	3.0	6.1

[a] BM and PM, blue membrane and purple membrane correspondingly. [b] pK_a of Asp-85 when group X is protonated. [c] pK_a of Asp-85 when group X is deprotonated. [d] Taken from ref *14*. [e] Taken from ref *34* and confirmed in this study.

At high pH, a second transition with pK_a ca. 9.1 is seen in the pH dependence of the DA in E194D, similar to that in the WT (Figure 8A) and E204D (Figure 8B). This transition is absent in the pH dependence of the DA of E194Q and E204N (Figure 8B), indicating that coupling between Asp-85 and the PRG is absent in these mutants. At neutral pH, the rate of the DA is very slow in the E194Q mutant, so it is difficult to detect.

In the framework of our model of the coupling of the pK_a's of Asp-85 and the PRG (*49*), the transition with pK_a ca. 9 should be attributed to the pK_a of the PRG X in the initial state of the pigment. From the pH dependence of the DA and the titration of Asp-85, we determined that upon protonation of Asp-85 the pK_a of this group decreases by 4.9 units in the WT (*49*), to 4.8 (see Table 1 and inset in Figure 8A). The magnitude of the change in the pK_a of one of the two interacting groups upon a change of the protonation state of the other group we call the *coupling strength*. As follows from the pH dependence of the DA, the coupling strength in the E194D mutant is 3.1 (6.1 − 3.0 = 9.1 − 6.0 = 3.1), 1.8 units less than in the WT. Upon deprotonation of the PRG in the ground state, the pK_a of Asp-85 increases from 3.0 to 6.1 whereas the pK_a of the PRG changes from 9.1 in the purple to 6.0 in the blue membrane. Thus, the decreased coupling strength between Asp-85 and the PRG X in the E194D mutant results in an elevated pK_a of X in the blue membrane (6 vs 4.8 in the WT) and a decreased pK_a of Asp-85 when the group X is deprotonated (6.1 vs 7.5 in the WT). These shifts of the pK_a's have implications for the pH dependence of proton release and the pH dependence of O decay. Thus, one would expect three results: (1) The pK_a of the PRG in M should be elevated to ca. 7.0 in this mutant (the difference of 1 pK unit is due to the effect of deprotonated Schiff base in M on the pK_a of the PRG; see refs *49*, *62*). The experimental value is 7.0 (*34*), so there is good agreement with this estimate. (2) If the idea that the pK_a of the PRG in O controls the lifetime of O is correct, then one should expect that the rate constant of the O → bR transition should have pK_a of about 5.5, assuming that, as for the WT, the pK_a of the PRG in O is 0.5−0.3 pK units less than the pK_a in the blue membrane (6.0 − 0.5 = 5.5). Again, this estimate is in good agreement with the experimental value of 5.3−5.6 (the latter value is obtained from simulation) (Figure 7B). (3) The pH dependence of the DA indicates that the pK_a of Asp-85 when the

PRG is deprotonated is 6.1 in E194D (vs 7.5 in WT). If one assumes that the pK_a of Asp-85 in O undergoes a similar shift, then one might expect to see a decrease in the accumulation of O intermediate at pH >6. This is exactly what is observed in the E194D mutant (Figure 7B). This correlation supports the notion that the pK_a of Asp-85 in O may be the factor affecting the accumulation of O (because of a faster deprotonation of Asp-85).

B. Titration of the E194Q Mutant: Slow Component in the Purple-to-Blue Transition. When the pH is decreased from 6 to 1, the absorption maximum of the dark-adapted E194Q shifts from 556 to 600 nm. A plot of the pH-induced absorption changes at 660 nm of E194Q due to the formation of the blue membrane results in a two-component titration curve with pK_a 3.1 (18%) and 2.5 with an unusually large *n* of 3 (Figure 8C). In E194Q gels, which were incubated for 24 h at room temperature, the pK_a of the titration curve is shifted to 3.1 and n is decreased to 2. A similar titration curve can be obtained in suspensions, but at elevated temperatures (35 °C). This indicates that the purple-to-blue transition (acid-induced protonation of Asp-85) has a very slow component in the E194Q mutant and that equilibrium is not reached on the time scale of usual titrations (tens of minutes) at 20 °C. The slow phases in the purple-to-blue transition are also present in the WT (*43*, *60*, and our unpublished results), but in E194Q, the rate of these slow phases is decreased severalfold more. A similar difference in the titration curves depending on time of incubation is also seen for the E194N, E204Q, and E204N mutants (data not shown). These observations suggest that the Glu-194 and Glu-204 residues strongly affect the transfer of protons not only from Asp-85 to the extracellular surface (*48*) but also from the bulk to Asp-85.

Effects of the E194Q and E204Q Mutations on the pH Dependence of O Formation and Decay. Figure 9A shows the kinetics of light-induced absorption changes at 660 nm in the E194Q mutant over the pH range of 8−5. The pH dependence of the maximal amplitude of O formation is shown in Figure 9C. Comparison of the data on the pH dependence of the O intermediate in the WT, E204Q, and E194Q mutants reveals several interesting features.

(1) The E194Q mutant does not show an increase of O amplitude with the pK_a 4 seen in the WT, and there is no substantial pH dependence in the rate of the O → bR transition at pHs below 6 (Figure 9B, curve 1). There is only a 2-fold decrease in the rate constant with pK_a of about 2.5; otherwise, the pH dependence of the rate constant is flat, similar to that in the E204Q mutant (Figure 9B, curve 2 and ref *48*). This indicates that the E194Q mutation largely eliminates the pH dependence of O decay, presumably by disabling the functioning of the PRG. This is similar to the result Richter et al. obtained for the E204Q mutant (*48*).

(2) Although the E204Q and E194Q mutations greatly slow the decay of the O intermediate and thus facilitate its accumulation at neutral pH in larger amounts than those of the WT, these mutations do not significantly affect the pH dependence of the maximum fraction of O intermediate (Figure 9C). In the WT and the mutants, the maximum fraction of O decreases with a similar pK_a, namely, 7.5 in the WT, 7.1 in E194Q, 7.7 in E204Q (Figure 9C), 7.2 in E194C, 7.3 in E194N, and 7.3 in the E204N mutants (data not shown for the last three). All pK_a's fall within a close

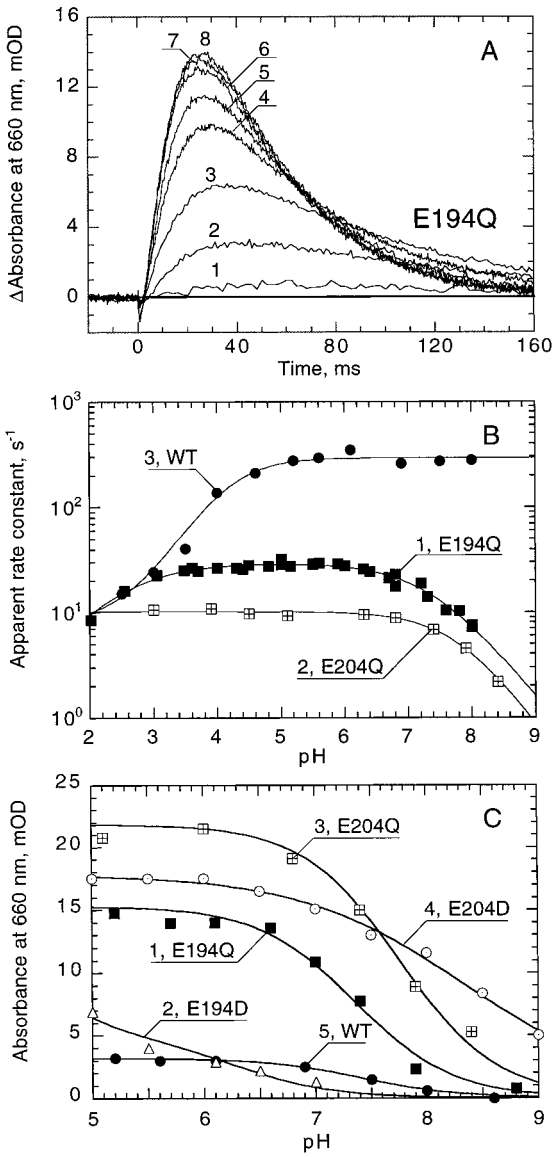

FIGURE 9: (A) Light-induced absorption changes at 660 nm in E194Q at different pHs: curves 1−8 at pH 8.3, 7.8, 7.3, 6.7, 6.3, 5.9, 5.5, and 5.0, respectively. (B) pH dependence of the rate constants of O decay in 1, E194Q; 2, E204Q; and 3, WT. (C) pH dependence of the maximum absorption changes at 660 nm in 1, E194Q; 2, E194D; 3, E204Q; 4, E204D; and 5, WT. Amplitudes are normalized to the same amount of M (20 mOD at 410 nm).

range, 7.1−7.7. From this, we conclude that the decrease in the fraction of O with pK_a ca. 7.5 is not directly associated with the PRG. The protonation state of some other residue might be involved in the control of this equilibrium. The most immediate candidate is Asp-96.

(3) Interestingly, in the E204D mutant, the pK_a of the maximum fraction of O intermediate is higher than those of the WT and other mutants (8.4) (Figure 9C). This mutant also shows a much larger fraction of O at neutral pH than E194D does. Thus, the conservative mutations in these two residues cause opposite effects on the maximum fraction of O intermediate at neutral pH and its pK_a. The E204D mutation stabilizes O (and the protonated state of Asp-85), but the E194D mutation causes the opposite effect. This correlates with the increased amount of the blue membrane in the E204D (see ref *34* and Figure 8B) at neutral pH and the decreased amount of blue membrane in E194D (Figure

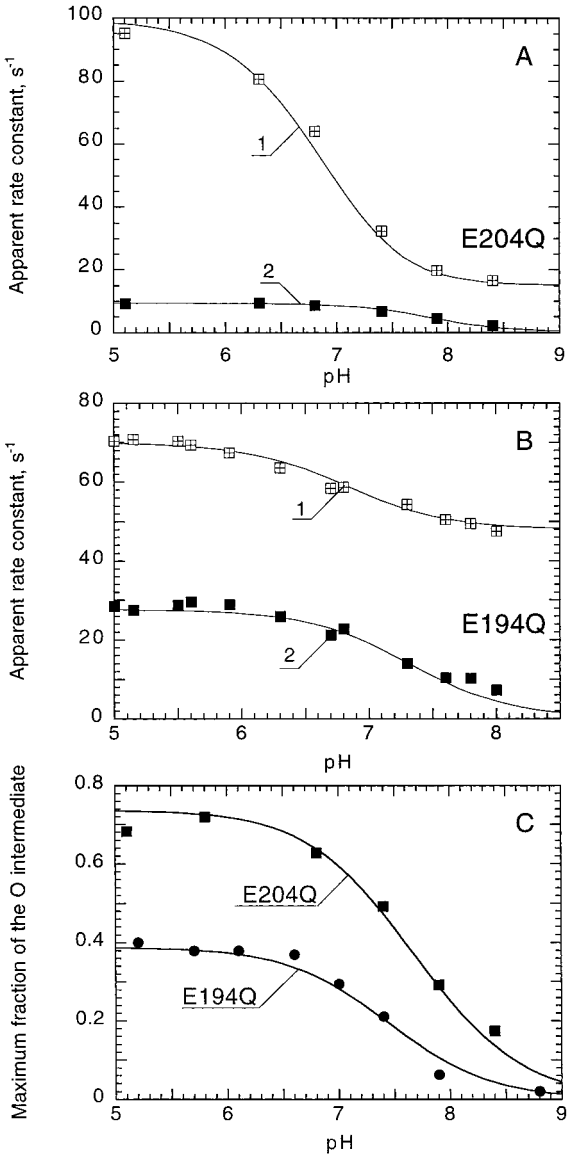

FIGURE 10: (A and B) pH dependencies of the apparent rate constants of O rise (1) and O decay (2) in E204Q (A) and E194Q (B), obtained from the fit of the light-induced absorption changes at 660 nm in 75 mM K_2SO_4 at 20 °C. Curves are fits of the experimental data with the N ⇔ O → bR model using eq 4 and assuming $k_1 = 95/(1 + 10^{pH-6.9})$ s^{-1}, $k_2 = 10$ s^{-1}, and $k_{-1} = 5$ s^{-1} for E204Q and $k_1 = 50/(1 + 10^{pH-7.1})$ s^{-1}, $k_2 = 39$ s^{-1}, and $k_{-1} = 9$ s^{-1} for E194Q. (C) pH dependencies of the fraction of the O intermediate in E204Q (1) and E194Q (2). Curves were generated with eqs 2′ and 3′ using the values for k_1, k_2, and k_{-1} listed above. Experimental data were normalized to a theoretical curve at the maximum (at pH 5.8).

8A), which can be interpreted as a shift in the equilibrium between Asp-85 and the proton release complex toward protonated Asp-85 in E204D and deprotonated Asp-85 in E194D (see Discussion).

(4) In the E204Q mutant, the apparent rate constant of O rise decreases with pK_a 6.9 whereas the rate constant of O decay decreases with pK_a 7.8 when the pH increases (Figure 10 A). Kinetic modeling indicates that these pH-dependent changes in the rate constants and in the fraction of O can be due to a single cause, namely, a decrease in the rate constant of the N → O transition when the pH is increased. Assuming that the rate constant of N → O has a pK_a 6.9 $k_1 = 95/(1 + 10^{pH-6.9})$ and that the rate constant of O decay is 10 s^{-1} at all pHs, we simulated the pH dependence of the maximum fraction of O intermediate using eqs 2 and 3. The calculated value is very close to the experimental one with pK_a 7.8 (Figure 10C). We also simulated the apparent rate constants of O rise and decay. The rate constants showed some deviation from the experimental values around pH 8.5. Including a back reaction from O → N with $k_{-1} = 5$ s^{-1} gives a good fit with eqs 2′ and 3′ (Figure 10A). Thus, the pH dependence of the fraction of O and of the rate constants of O rise and decay in the E204Q mutant can be explained assuming the pH dependence of the rate constant of the N → O transition with pK_a 6.9.

The E194Q mutant shows a weaker pH dependence of the apparent rate constant of O rise compared to that of the E204Q mutant (compare curves 1 in parts A and B of Figure 10). However, the pH dependencies of the maximum fraction of O intermediate are similar (Figure 10C). As in the case of E204Q, the apparent time constants and the pH dependence of the fraction of O can be simulated (parts B and C of Figure 10) if it is assumed that k_1 is pH-dependent with pK_a 7.1, the O → bR transition is not pH-dependent ($k_2 = 39$ s^{-1}), and there is a back reaction from O to N ($k_{-1} = 9$ s^{-1}).

An interesting question is whether the pH dependence of the N → O reaction is controlled by the proton uptake (and presumably reprotonation of Asp-96). The kinetics of proton uptake in E204Q (*30*, *31*, *41*), E194C (*33*), and E194Q (*34*) coincide with the N → O transition. These data are in agreement with the view that the rate of the N → O transition is controlled by proton uptake from the cytoplasmic side of the membrane to reprotonate Asp-96 (*17*, *19*, *20*) directly or through intermediate groups such as Asp-38 (see ref *61*).

(5) Azide and weak acids such as formate and cyanate accelerate both the decay of the O intermediate and proton release in the E204Q mutant to a rate similar to that in the WT (*41*). The same is true for the E194C (Figure 11) and E194Q (data not shown) mutants. The addition of 100 mM azide results in a decrease of the lifetime of the O intermediate from 60 to 20 ms. Azide accelerates not only O decay but also M decay and O rise (as one can conclude from the fit of the traces in Figure 11). This is different from the E204Q mutant where N → O transition is faster (95 s^{-1} vs 50 s^{-1} in E194Q) and is not affected significantly by azide (*41*). Thus, a slower N → O transition and its acceleration by azide in E194Q and E194C mutants indicate that these mutations produce a defect that affects not only proton release but (to a lesser extent) proton uptake at the cytoplasmic side. It is possible that neutralization (protonation) of Glu-194 at low pH in WT can cause a similar defect; that would explain the sensitivity of WT to azide at low pH (Figure 4).

DISCUSSION

A Group with pK_a 4.3−4.5 That Catalyzes the O → bR Transition in the WT Can Be Identified as PRG. When the pH decreases, the rate constant of O decay in the WT decreases with a pK_a of about 4.3, indicating that deprotonation of some group in O facilitates deprotonation of Asp-85. Increased protonation of this group at low pH results in a slowing of O decay (Figures 1 and 2) and an increase in the maximum fraction of O (Figure 3A). The decay of O

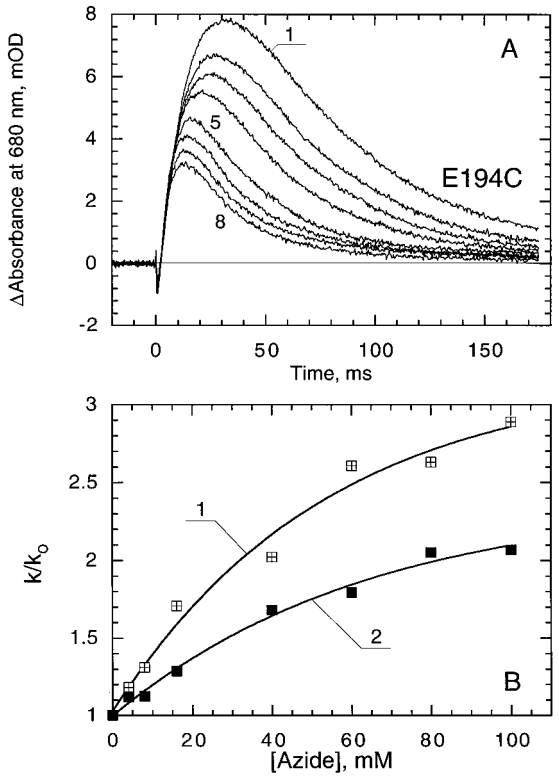

FIGURE 11: Effect of azide on light-induced absorption changes in E194C at pH 5.0. (A) Kinetics of absorption changes at 680 nm due to O formation and decay. Curves 1−8 correspond to 0, 5, 10, 15, 40, 60, 80, and 100 mM azide. (B) Apparent rate constants of O rise (1) and O decay (2) as a function of the concentration of azide. At 20 °C, the rate constant in the absence of azide, k_0, is equal to 59 s^{-1} for O rise and 19 s^{-1} for O decay.

can be accelerated by azide in the WT and the mutants, presumably by restoring the proton transfer in the channel, and it can be slowed by D_2O (Figure 5). The latter indicates that proton-transfer reactions are the rate-limiting steps in the O → bR transition at low pH. Fitting kinetics of O formation and decay shows that at neutral pH the rate constant of the O → bR transition in the WT is at least 30 times faster than that in the E204Q mutant where the PRG is disabled. At pH 3, the rate constants are similar.

The most logical candidate for the group with pK_a 4.3 in the O state is the PRG, a complex of residues which includes Glu-204, Glu-194, and one or more water molecules that are hydrogen-bonded to these residues, particularly the water molecule W403 between Arg-82 and Glu-204 (*39*). Mutation of any of these residues eliminates fast proton release (*28, 31, 33, 34*), indicating that all components are important. According to one view, these residues are organized into a hydrogen-bonded network that shares the proton (*35*). Alternatively, the roles of these residues might be different, and Glu-194 could be the residue that actually releases the proton (*34*). In our earlier studies, we have established that a group X′ is present that interacts with Asp-85 in such a way that protonation states of Asp-85 and X′ are strongly coupled (*28, 49, 62*). When X′ deprotonates (with pK_a 9.7 in the unphotolyzed state), the pK_a of Asp-85 increases from 2.6 to 7.5. Conversely, when Asp-85 is protonated (in the blue membrane), the pK_a of the group X′ is decreased from 9.7 to 4.8 (see Table 1 and inset in Figure 8A). The latter property makes X′ a very plausible candidate for the PRG (*9, 14*). This group has a pK_a of about 5.8 in the M intermediate of the WT (*14*). The coupling model (*28, 49*) was successfully used to explain and predict the pH dependence of proton release and other features of several mutants of bR (*28, 33, 34, 62*−*65*). These studies support the hypothesis that X′ and X are the same group. The difference of ca. 1 p*K* unit between the lower pK_a's of X in M (5.8) and X' in the blue membrane (4.8) was attributed to the different protonation states of the Schiff base in the blue membrane (protonated) and in M (deprotonated) (*49, 62*).

It is reasonable to apply the coupling model to estimate the pK_a of the PRG in the O intermediate because this intermediate is even more similar to the blue membrane than the M intermediate. The pK_a of X' in the blue membrane of 4.8 is close to the value we obtained for the pK_a of the group controlling proton release from Asp-85 in the O intermediate (4.3−4.5). The difference between the two values probably is due to differences in the structures of the blue membrane and the O intermediate. There is also a possibility that at neutral pH $k_{O\rightarrow bR}$ is somewhat faster than the fast component of the M → N transition at neutral pH, k_{MN} (*19, 20, 55*). In this case, simulation of the kinetics of the photocycle reactions using a more complete model (M ⇔ N ⇔ O → bR) results in a slightly larger pK_a for the O → bR transition, 4.5−4.6, which is in a closer agreement with the 4.8 value found for the blue membrane. Thus, we conclude that in the WT the O → bR transition (and the deprotonation of Asp-85) slows at low pH because of the decreased deprotonation of the PRG which in the protonated state cannot accept a proton from Asp-85. This indicates that proton release from Asp-85 to the surface at low pH occurs through the PRG as at neutral pH.

Experiments with the E194D mutant support this conclusion. In this mutant, the pK_a's of the PRG both in the M state and in the blue membrane, as well as for the rate constant of the O → bR transition, are all ca. 1.2 p*K* units higher than in the WT (see Table 1). This can be explained by assuming that the PRG is responsible for the pH dependence of O decay. Finally, the absence of the pH dependence of O decay in the E204Q and E194Q mutants is also in agreement with this conclusion.

Implications of the Proton Exchange between Asp-85 and the Extracellular Surface Being through the PRG. If one assumes that the proton movement from Asp-85 to the extracellular surface occurs mainly through the PRG X (when this group is functional, as in WT), then obviously the pK_a of Asp-85 becomes dependent on the pK_a of X. Here, we briefly consider a version of the coupling model (*28, 49*) that emphasizes that proton exchange of Asp-85 with extracellular surface occurs through the PRG. The latter has different pK_a's depending on whether Asp-85 is deprotonated (pK_{a1}) or protonated (pK_{a3}):

$$\underset{\text{state 1}}{D85^- X^-} \overset{pK_{a1}}{\underset{H^+}{\rightleftharpoons}} \underset{\text{state 2}}{D85^- XH} \overset{pK_2}{\rightleftharpoons} \underset{\text{state 3}}{D85H X^-} \overset{pK_{a3}}{\underset{H^+}{\rightleftharpoons}} \underset{\text{state 4}}{D85H XH}$$

In this model, pK_2 defines the equilibrium constant of intramolecular proton exchange between Asp-85 and the PRG X. The apparent pK_a of Asp-85 depends on the state of group X. At high pH, the proton exchange of Asp-85 with the extracellular surface occurs through state 1 where group X is deprotonated. The apparent pK_a of Asp-85 can be

calculated as a sum of pK_{a1} and pK_2. At low pH, proton exchange occurs through state 4, and the apparent pK_a of Asp-85 can be calculated as a sum of pK_2 and pK_{a3}. The fraction of blue membrane for this model is given by the equation:

$$f_{DH} = \alpha/(\alpha + \beta\gamma) \quad (5)$$

where $\alpha = 1 + 10^{pK_{a3}-pH}$, $\beta = 1 + 10^{pH-pK_{a1}}$, and $\gamma = 10^{-pK_2}$. The fit of the pH dependence of the DA in the WT with this formula gives the following values: pK_{a1} = 9.6, pK_2 = −2.2, and pK_{a3} = 4.8. Equation 5 is a different but equivalent form of a previously derived formula (*49*). Because it is derived for equilibrium conditions, the assumption of direct or indirect (through the PRG) proton exchange of Asp-85 with the extracellular surface does not effect the pK_a's. Equation 5 emphasizes the pK of proton exchange between Asp-85 and the PRG (pK_2) as an important parameter. In the WT, pK_2 is equal to −2.2, indicating that the equilibrium is shifted toward deprotonated Asp-85 (purple membrane) with a ratio of purple/blue of more than 100:1. This can be seen directly from the pH dependence of the DA curve (Figure 8), which is proportional to the fraction of protonated Asp-85. In the E194D mutant, the equilibrium is even more shifted toward deprotonation of Asp-85, by a factor of 1000:1 (pK_2 = −3). On the contrary, in the E204D mutant, the ratio of the purple to blue species at neutral pH is close to 10:1 (p$K_2 \approx -1$). When pK_2 is close to 0, a large amount of blue membrane at neutral pH is present, as in the D85E mutant (*62, 64*). Thus, the interaction of Asp-85 with the PRG is an important aspect of proton transfer in bR that can be characterized by a value of pK_2.

On the pH Dependence of the N ⇔ O Equilibrium. The N ⇔ O equilibrium has a very strong pH dependence around neutral pH: the O intermediate accumulates at low pH but does not accumulate at high pH. The fraction of O decreases with a pK_a of about 7.2−7.5 in the WT (Figure 3A and earlier data in refs *21*, *47*). Obviously, protonation of some residue controls this transition. Cao et al. (*21*) discussed the nature of this transition and suggested that the fraction of O intermediate might be controlled by (i) the rate of proton uptake or (ii) the pK_a of the PRG in M which affects branching of the photocycle into two pathways differing in the order of proton uptake and release and supposedly relative fractions of the N and O intermediates (*21*). The latter possibility was tested in this study using the E204Q and E194Q mutants. Because fast proton release is abolished in these mutants, one would expect that the equilibrium between N and O would be altered if the fast proton release plays any role in the control of the N ⇔ O equilibrium. The data obtained in this study clearly show that the pH dependencies of the maximum fractions of O have similar pK_a's in the range of 7.1−7.7, in the WT, E194Q, and E204Q mutants, as well as in E194C (*51*). Thus, we conclude that the elimination of fast proton release during the L → M transition does not affect the pK_a of the N ⇔ O equilibrium (the pH dependence of the fraction of O).

Moreover, the pH dependence of the apparent rate constants of O rise and decay in E204Q and E194Q and the pH dependence of the maximum fraction of O (Figure 10) can be explained by the assumption that it is the decrease in the rate constant of the N → O transition and proton uptake which causes the decrease in the fraction of O. In the WT, the decrease in the fraction of O intermediate can be explained in a similar way (Figure 3C and ref *20*). This implies that proton uptake and reprotonation of Asp-96 is a prerequisite for O formation and apparently for the 13-*cis*/all-*trans* isomerization during the N → O transition.

Rothschild et al. (*22*) suggested that decay of the N intermediate may be controlled by reprotonation of Asp-96. Zscherp and Heberle (*66*) reported that the pK_a of Asp-96 is 7.2 in N, which agrees with an earlier suggestion (*67*). If one assumes that the N → O transition occurs upon protonation of Asp-96 and that the pK_a of Asp-96 in N is 7.2, then at high pH the rate of the N → O transition should be slow due to the decrease in the fraction of protonated Asp-96. The simplest model, N + H^+ ⇔ O → bR, can account for the observed pH dependence of the kinetics of O formation and decay in E204Q and E194Q. The model which can also account for the decrease in the fraction of O accumulated is the one that suggests that the protonation of Asp-96 occurs already in the N intermediate: N_1 ($D96^-$) + H^+ ⇔ N_2 (D96H) ⇔ O → bR. The existence of two N forms differing in the protonation of Asp-96 was suggested earlier (*20, 68*). These models do not require the N → bR branch in the cycle to account for decrease in the amount of O formed.

The fraction of O is controlled also by the rate of deprotonation of Asp-85. It is well-established that Asp-85 is protonated in O (*19, 32, 66, 69*). Thus, if Asp-85 deprotonate with a rate constant substantially faster than the rate constant of O formation, then no O will accumulate. Measurements by Richter et al. (*48*) indicate that the deprotonation of Asp-85 at pH 7 takes place in 3 ms in the WT and 25 ms in E204Q. The time constant of O decay is also ca. 3 ms (see Figure 2B) or less (if the apparent constant is limited by the rate of the M → N transition). The FTIR data showed that the pK_a of Asp-85 is very high in M (*70*) and N (*25*). During the M → N transition, a shift of the frequency of the Asp-85 carboxyl band takes place (*25*), indicating a change of environment around the carboxyl of Asp-85, but the residue still remains protonated even at pH 10. The pK_a of Asp-85 in the O intermediate has not been determined directly. It might be estimated as 7.5 for the WT, if one assumes that the pK_a of Asp-85 in O is close to the pK_a of Asp-85 in the blue membrane when the PRG is deprotonated. The pH dependence of the fraction of blue membrane in WT indicates that, upon deprotonation of the PRG, the pK_a of the Asp-85 increases to 7.5; see ref *49*. This can provide an explanation for the decrease in the fraction of O in the WT, because proton transfer between Asp-85 and the PRG occurs rapidly. However, in the E204Q and E194Q mutants, the PRG is disabled and deprotonation of Asp-85 occurs very slowly. For these cases, the major factor determining the pH dependence of the fraction of O is the rate of the N → O reaction and the rate of proton uptake coupled to this transition. The latter depends on the pK_a of the group which undergoes reprotonation (Asp-96). If one assumes that the deprotonation of Asp-85 can occur relatively independently from the reprotonation of Asp-96, then at high pH, when the reprotonation of Asp-96 is dramatically slowed, the deprotonation of Asp-85 and proton release may occur first (in the N intermediate), followed by proton uptake, which is exactly what was found for the

E194Q and E204Q mutants at high pH (*71*). This interpretation suggests a pH-dependent branching (presumably in N). In the E194D mutant, the fast deprotonation of Asp-85 decreases fraction of O at neutral pH and thus affects the pH dependence of the fraction of O. Further studies are necessary to determine the pK_a of Asp-85 in the N and O intermediates in different mutants and to investigate the possibility of the contribution of the deprotonation of Asp-85 in N into the kinetics of photocycle reactions and the pH dependence of the fractions of the N and O intermediates.

In conclusion, in the WT, the rate constant of the O → bR transition decreases at low pH with a pK_a of about 4.5 leading to an accumulation of the O intermediate. We conclude that this pK_a is the pK_a of the PRG in O. The O → bR transition is slowed because proton transfer from Asp-85 to the PRG cannot take place until the group is deprotonated. At high pH, the N → O transition slows, with the pK_a of about 7.5 probably due to the slowing of the reprotonation of Asp-96. The relative rates of the Asp-96 reprotonation and Asp-85 deprotonation in the N → O → bR transitions determine the fraction of O accumulated.

ACKNOWLEDGMENT

The authors are grateful to Dr. A. Maeda for reading the manuscript and providing helpful discussion.

REFERENCES

1. Oesterhelt, D., and Stoeckenius, W. (1973) *Proc. Natl. Acad. Sci. U.S.A. 70*, 2853−2857.
2. Birge, R. R. (1990) *Biochim. Biophys. Acta 1016*, 293−327.
3. Mathies, R. A., Lin, S. W., Ames, J. B., and Pollard, W. T. (1991) *Annu. Rev. Biophys. Biophys. Chem. 20*, 491−518.
4. Rothschild, K. J. (1992) *J. Bioenerg. Biomembr. 24*, 147−167.
5. Oesterhelt, D., Tittor, J., and Bamberg, E. (1992) *J. Bioener. Biomembr. 24*, 181−191.
6. Khorana, H. G. (1993) *Proc. Natl. Acad. Sci. U.S.A. 90*, 1166−1171.
7. El-Sayed, M. (1993) *Acc. Chem. Res. 25*, 279−286.
8. Lanyi, J. K. (1993) *Biochim. Biophys. Acta 1183*, 241−261.
9. Ebrey, T. G. (1993) in *Thermodynamics of Membranes, Receptors and Channels* (Jackson, M., Ed.) pp 353−387, CRC Press, Boca Raton, FL.
10. Ottolenghi, M., and M. Sheves., Eds. (1995) Photophysics and Photochemistry of Retinal Proteins. *Isr. J. Chem. 34*, 193−513 (a collection of review papers).
11. Lanyi, J. K. (1997) *J. Biol. Chem. 272*, 31209−31212.
12. De Groot, H. J. M., Smith, S. O., Courtin, J., van den Berg, E., Winkel, C., Lugtenburg, J., Griffin, R. G., and Herzfeld, J. (1990) *Biochemistry 29*, 6873−6883.
13. Siebert, F., Mäntele, W., and Kreutz, W. (1982) *FEBS Lett. 141*, 82−87.
14. Zimányi, L., Váró, G., Chang, M., Ni, B., Needleman, R., and Lanyi, J. K. (1992) *Biochemistry 31*, 8535−8543.
15. Dencher, N., and Wilms, M. (1975) *Biophys. Struct. Mech. 1*, 259−271.
16. Drachev, L. A., Kaulen, A. D., Skulachev, V. P., and Zorina, V. V. (1987) *FEBS Lett. 226*, 139−144.
17. Otto, H., Marti, T., Holtz, M., Mogi, T., Lindau, M. H., Khorana, G., and Heyn, M. P. (1989) *Proc. Natl. Acad. Sci. U.S.A. 86*, 9228−9232.
18. Henderson, R., Baldwin, J. M., Ceska, T. A., Zemlin, F., Beckmann, E., and Downing, K. H. (1990) *J. Mol. Biol. 213*, 899−929.
19. Souvignier, G., and Gerwert, K. (1992) *Biophys. J. 63*, 1393−1405.
20. Ames, J. B., and Mathies, R. (1990) *Biochemistry 29*, 7181−7190.
21. Cao, Y., Brown, L. S., Needleman, R., and Lanyi, J. K. (1993) *Biochemistry 32*, 10239−10248.
22. Rothschild, K. J., Marti, T., Sonar, S., He, Y.-W., Rath, P., Fischer, W., and Khorana, H. G. (1993) *J. Biol. Chem. 268*, 27046−27052.
23. Brown, L. S., Váró, G., Needleman, R., and Lanyi, J. K. (1995) *Biophys. J. 69*, 2103−2111.
24. Fodor, S. P. A., Ames, J. B., Gebhard, R., van den Berg, E. M. M., Stoeckenius, W., Lugtenburg, J., and Mathies, R. (1988) *Biochemistry 27*, 7097−7101.
25. Pfefferlé, J.-M., Maeda, A., Sasaki, J., and Yoshizawa, T. (1991) *Biochemistry 30*, 6548−6556.
26. Smith, S. O., Pardoen, J. A., Mulder, P. P. J., Curry, B., Lugtenburg, J., and Mathies, R. A. (1983) *Biochemistry 22*, 6141−6148.
27. Zscherp, C., and Heberle, J. (1997) *J. Phys. Chem. 101*, 10542−10547.
28. Balashov, S. P., Govindjee, R., Kono, M., Imasheva, E., Lukashev, E., Ebrey, T. G., Crouch, R. K., Menick, D. R., and Feng, Y. (1993) *Biochemistry 32*, 10331−10343.
29. Brown, L. S., Bonet, L., Needleman, R., and Lanyi, J. K. (1993) *Biophys. J. 65*, 124−130.
30. Govindjee, R., Misra, S., Balashov, S. P., Ebrey, T. G., Crouch, R. K., and Menick, D. R. (1996) *Biophys. J. 71*, 1011−1023.
31. Brown, L. S., Sasaki, J., Kandori, H., Maeda, A., Needleman, R., and Lanyi, J. K. (1995) *J. Biol. Chem. 270*, 27122−27126.
32. Kandori, H., Yamazaki, Y., Hatanaka, M., Needleman, R., Brown, L. S., Richter, H.-T., Lanyi, J. K., and Maeda, A. (1997) *Biochemistry 36*, 5134−5141.
33. Balashov, S. P., Imasheva, E. S., Ebrey, T. G., Chen, N., Menick, D. R., and Crouch, R. K. (1997) *Biochemistry 36*, 8671−8676.
34. Dioumaev, A. K., Richter, H.-T., Brown, L. S., Tanio, M., Tuzi, S., Saito, H., Kimura, Y., Needleman, R., and Lanyi, J. K. (1998) *Biochemistry 37*, 2496−2506.
35. Rammelsberg, R., Huhn, G., Lubben, M., and Gerwert, K. (1998) *Biochemistry 37*, 5001−5009.
36. Grigorieff, N., Ceska, T. A., Downing, K. H., Baldwin, J. M., and Henderson, R. (1996) *J. Mol. Biol. 259*, 393−421.
37. Kimura, Y., Vassylyev, D. G., Miyazawa, A., Kidera, A., Matsushima, M., Mitsuoka, K., Murata, K., Hirai, T., and Fujiyoshi, Y. (1997) *Nature 389*, 206−211.
38. Pebay-Peyroula, E., Rummel, G., Rosenbusch, J. R., and Landau, E. M. (1997) *Science 277*, 1676−1681.
39. Luecke, H., Richter, H.-T., and Lanyi, J. K. (1998) *Science 280*, 1934−1937.
40. Essen, L. O., Siegert, R., Lehmann, W. D., and Oesterhelt, D. (1998) *Proc. Natl. Acad. Sci. U.S.A. 95*, 11673−11678.
41. Misra, S., Govindjee, R., Ebrey, T. G., Chen, N., Ma, J.-X., and Crouch, R. K. (1997) *Biochemistry 36*, 4875−4883.
42. Lozier, R. H., and Niederberger, W. (1977) *Fed. Proc. 36*, 1805−1809.
43. Moore, T. A., Edgerton, M. E., Parr, G., Greenwood, C., and Perham, R. N. (1978) *Biochem. J. 171*, 469−476. Edgerton, M. E., Moore, T. A., and Greenwood, C. (1980) *Biochem. J. 189*, 413−420.
44. Stoeckenius, W., Lozier, R. H., and Bogomolni, R. A. (1979) *Biochim. Biophys. Acta 505*, 215−278.
45. Li, Q., Govindjee, R., and Ebrey, T. G. (1984) *Proc. Natl. Acad. Sci. U.S.A. 81*, 7079−7082.
46. Lozier, R., Xie, A., Hofrichter, J., and Clore, G. M. (1992) *Proc. Natl. Acad. Sci. U.S.A. 89*, 3610−3614.
47. Eisfeld, W., Pusch, C., Diller, R., Lohrmann, R., and Stockburger, M. (1993) *Biochemistry 32*, 7196−7215.
48. Richter, H.-T., Needleman, R., Kandori, H., Maeda, A., and Lanyi, J. K. (1996) *Biochemistry 35*, 15461−15466.
49. Balashov, S. P., Imasheva, E. S., Govindjee, R., and Ebrey, T. G. (1996) *Biophys. J. 70*, 473−481.
50. Lanyi, J. K., and Váró, G. (1995) *Isr. J. Chem. 35*, 365−385.
51. Balashov, S. P., Imasheva, E. S., Govindjee, R., Ebrey, T. G., Chen, N. D., Menick, R., and Crouch, R. K. (1998) *Biophys. J. 74*, 2, 293a.
52. Becher, B., and Cassim, J. Y. (1975) *Prepr. Biochem. 5*, 161−178.

53. Govindjee, R., Balashov, S. P., and Ebrey, T. G. (1990) *Biophys. J. 58*, 597−608.
54. Liu, S. Y., Kono, M., and Ebrey, T. G. (1991) *Biophys. J. 60*, 204−216.
55. Gillbro, T. (1978) *Biochim. Biophys. Acta 504*, 175−186.
56. Chizhov, I., Chernavskii, D. S., Engelhard, M., Mueller, K.-H., Zubov, B. V., and Hess, B. (1996) *Biophys. J. 71*, 2329−2345.
57. Tittor, J., Wahl, M., Schweiger, U., and Oesterhelt, D. (1994) *Biochim. Biophys. Acta 1187*, 191−197.
58. Le Coutre, J., and Gerwert, K. (1996) *FEBS Lett. 398*, 333−336.
59. Váró, G., and Lanyi, J. K. (1990) *Biochemistry 29*, 2241−2250.
60. Friedman, N., Rousso, I., Sheves, M., Fu, X., Bressler, S., Druckmann, S., and Ottolenghi, M. (1997) *Biochemistry 36*, 11369−11380.
61. Riesle, J., Oesterhelt, D., Dencher, N. A., and Heberle, J. (1996) *Biochemistry 35*, 6635−6643.
62. Balashov, S. P., Govindjee, R., Imasheva, E. S., Misra, S., Ebrey, T. G., Feng, Y., Crouch, R. K., and Menick, D. R. (1995) *Biochemistry 34*, 8820−8834.
63. Richter, H.-T., Brown, L. S., Needleman, R., and Lanyi, J. K. (1996) *Biochemistry 35*, 4054−4062.
64. Richter, H. T., Needleman, R., and Lanyi, J. K. (1996) *Biophys. J. 71*, 3392−3398.
65. Balashov, S. P., Imasheva, E. S., Govindjee, R., Sheves, M., and Ebrey, T. G. (1996) *Biophys. J. 71*, 1973−1984.
66. Zscherp, C., and Heberle, J. (1997) *Biophys. J. 72*, part 2, A206.
67. Cao, Y., Váró, G., Klinger, A. L., Czajkowsky, D. M., Braiman, M. S., Needleman, R., and Lanyi, J. K. (1993) *Biochemistry 32*, 1981−1990.
68. Zimányi, L., Cao, Y., Needleman, R., Ottolenghi, M., and Lanyi, J. K. (1993) *Biochemistry 32*, 7669−7678.
69. Hessling, B., Souvignier, G., and Gerwert, K. (1993) *Biophys. J. 65*, 1929−1941.
70. Braiman, M. S., Dioumaev, A. K., and Lewis, J. R. (1996) *Biophys. J. 70*, 939−947.
71. Koyama, K., Miyasaka, T., Needleman, R., and Lanyi, J. K. (1998) *Photochem. Photobiol. 68*, 400−406.

BI981926A